

A First-Occupancy Representation for Reinforcement Learning

Ted Moskovitz^{*1}, Spencer R. Wilson², Maneesh Sahani¹

¹Gatsby Unit, UCL ²Sainsbury Wellcome Centre, UCL

Abstract

Both animals and artificial agents benefit from state representations that support rapid transfer of learning across tasks and which enable them to efficiently traverse their environments to reach rewarding states. The *successor representation* (SR), which measures the expected cumulative, discounted state occupancy under a fixed policy, enables efficient transfer to different reward structures in an otherwise constant Markovian environment and has been hypothesized to underlie aspects of biological behavior and neural activity. However, in the real world, rewards may move or only be available for consumption once, may shift location, or agents may simply aim to reach goal states as rapidly as possible without the constraint of artificially imposed task horizons. In such cases, the most behaviorally-relevant representation would carry information about when the agent was likely to *first* reach states of interest, rather than how often it should expect to visit them over a potentially infinite time span. To reflect such demands, we introduce the *first-occupancy representation* (FR), which measures the expected temporal discount to the first time a state is accessed. We demonstrate that the FR facilitates the selection of efficient paths to desired states, allows the agent, under certain conditions, to plan provably optimal trajectories defined by a sequence of subgoals, and induces similar behavior to animals avoiding threatening stimuli.

1 Introduction

In order to maximize reward, both animals and machines must quickly make decisions in uncertain environments with rapidly changing reward structure. Often, the strategies employed by these agents are categorized as either model-free (MF) or model-based (MB) learning (Sutton & Barto, 2018). In the former, the optimal action in each environmental state is identified through trial and error, with propagation of learnt value from state to state. By contrast, the latter depends on the acquisition of a map-like representation of the transition structure of an environment, from which an optimal course of action may be derived as needed. The two schemes offer competing advantages. MF behaviour requires little computation during execution, but depends on extensive experience in a constant environment with unchanging objectives and so is slow to adapt to modifications in the environment or new goals. MB action can flexibly adapt to changes in environment or objectives, but at the cost of considerable computational effort in planning and the risk of mismatches between the model and the real world significantly hurting performance (Azar et al., 2013).

This sharp dichotomy has motivated a search for intermediate models which cache information about environmental structure, and so enable efficient but flexible planning. One such approach, based on the *successor representation* (SR) (Dayan, 1993), has been the subject of recent interest in the context of both biological (Stachenfeld et al., 2017; Gershman, 2018; Momennejad et al., 2017; Vértés & Sahani, 2019; Behrens et al., 2018) and machine (Kulkarni et al., 2016; Barreto et al., 2017b;a; 2018; Machado et al., 2020; Ma et al., 2020; Madarasz & Behrens, 2019) learning. The SR associates with each state and policy of action a measure of the expected rate of future occupancy of all states if that policy were to be followed indefinitely. This cached representation makes it possible to rapidly evaluate the expected return of each available policy for any distribution of reward in an otherwise unchanging environment, provided that this reward distribution remains stationary throughout an episode. The SR can be acquired through experience in much the same way as MF methods and provides some of the flexibility of MB behaviour at much reduced computational cost.

However, the requirements that reward distributions be static and that environments remain entirely unchanged limits the applicability of the SR. In the real world, rewards may be depleted by consumption, frequently

^{*}email: ted@gatsby.ucl.ac.uk

only being available on the first entry to each state. Internal goals for control—say, to pick up a particular object—need to be achieved as accurately and rapidly as possible, but only once at a time. To flexibly model such settings requires a violation of the common Markovian assumption that underlies the SR. If a goal is rewarded only when first achieved, then a Markov model requires an updated transition structure to reflect the subsequent lack of reward if the state is revisited. If goals move then one needs a different Markov model for each, violating the environmental stationarity required by the SR.

Furthermore, an SR is associated with a single policy of action. A collection of SRs for different policies makes it possible to select the best amongst them, or to improve upon them all by considering the best policy-dependent values of states accessible after taking a single action in the current state (Barreto et al., 2018). But this capacity still falls far short of the power of planning within complete models of the environment.

Here, we propose a different form of representation in which the information cached is appropriate to achieving ephemeral rewards and to planning complex combinations of policies to achieve one-off goals. Both features arise from considering the expected time at which other states will be *first* accessed by following the policies available from each initial state. We refer to this as a *first-occupancy representation* (FR). The shift from expected rate of future occupancy (SR) to delay to first occupancy makes it possible to handle settings where the underlying environment remains stationary, but reward availability is not Markovian. Furthermore, it enables an effective form of planning based on transitions between policies when specific states are accessed at arbitrary times in the future. We demonstrate that this method of planning produces behavior that is similar to that of animals under pressure to produce efficient trajectories through their environment. We hope the FR serves as a foundation for future work, as well as inspires new approaches to learning effective representations for real-world tasks.

2 Reinforcement Learning Preliminaries

Policy evaluation and improvement In reinforcement learning (RL), the goal of the agent is to act so as to maximize the discounted cumulative reward received within a task-defined environment. Typically, task T is modelled as a finite *Markov decision process* (MDP; (Puterman, 2010)), $T = (\mathcal{S}, \mathcal{A}, p, r, \gamma, \mu)$, where \mathcal{S} is a finite state space, \mathcal{A} is a finite action space, $p : \mathcal{S} \times \mathcal{A} \rightarrow \Delta(\mathcal{S})$ is the transition distribution (where $\Delta(\mathcal{S})$ is the probability simplex over \mathcal{S}), $r : \mathcal{S} \rightarrow \mathbb{R}$ is the reward function, $\gamma \in [0, 1)$ is a discount factor, and $\mu \in \Delta(\mathcal{S})$ is the distribution over initial states. We will often consider problems with a fixed initial state s_0 , meaning that the support of μ is restricted to s_0 . Note that the reward function is also frequently defined over state-action pairs (s, a) or triples (s, a, s') , but we restrict our analysis to state-based rewards for now. The goal of the agent is to maximize its expected *return*, or discounted cumulative reward $\sum_t \gamma^t r(s_t)$. To simplify notation, we will frequently write $r(s_t) := r_t$ and $\mathbf{r} \in \mathbb{R}^{|\mathcal{S}|}$ as the vector of rewards for each state. The agent acts according to a stationary policy $\pi : \mathcal{S} \rightarrow \Delta(\mathcal{A})$. For finite MDPs, we can describe the expected transition probabilities under π using a $|\mathcal{S}| \times |\mathcal{S}|$ matrix P^π such that $P_{s,s'}^\pi = p^\pi(s'|s) := \sum_a p(s'|s, a)\pi(a|s)$. Given a reward function r , the expected return for policy π is

$$Q_r^\pi(s, a) = \mathbb{E}_\pi \left[\sum_{k=0}^{\infty} \gamma^k r_{t+k} \mid s_t = s, a_t = a \right] = \mathbb{E}_{s' \sim p^\pi(\cdot|s)} [r_t + \gamma Q_r^\pi(s', \pi(s'))]. \quad (1)$$

Q_r^π are called the state-action values or simply the Q -values of π . The expectation $\mathbb{E}_\pi[\cdot]$ is taken with respect to the randomness of both the policy and the transition dynamics. For simplicity of notation, from here onwards we will write expectations of the form $\mathbb{E}_\pi[\cdot \mid s_t = s, a_t = a]$ as $\mathbb{E}_\pi[\cdot \mid s_t, a_t]$. This recursive form is called the *Bellman equation*, and it makes the process of estimating Q_r^π —termed *policy evaluation*—tractable via dynamic programming (DP; (Bellman, 1957)). In particular, successive applications of the *Bellman operator* $\mathcal{T}^\pi Q := r + \gamma P^\pi Q$ are guaranteed to converge to the true value function Q^π for any initial real-valued $|\mathcal{S}| \times |\mathcal{A}|$ matrix Q .

When the transition dynamics and reward function are unknown, *temporal difference* (TD) learning updates value estimates using a bootstrapped estimate of the Bellman target (Sutton & Barto, 2018). Given a transition sequence (s_t, a_t, r_t, s_{t+1}) and $a_{t+1} \sim \pi(\cdot|s_{t+1})$,

$$Q_r^\pi(s_t, a_t) \leftarrow Q_r^\pi(s_t, a_t) + \alpha \delta_t, \quad \delta_t := r_t + \gamma Q_r^\pi(s_{t+1}, a_{t+1}) - Q_r^\pi(s_t, a_t). \quad (2)$$

Once a policy has been evaluated, *policy improvement* identifies a new policy π' such that $Q_r^{\pi'}(s, a) \geq$

$Q_r^{\pi'}(s, a), \forall (s, a) \in Q_r^\pi(s, a)$. Helpfully, such an improved policy can be defined as

$$\pi'(s) \in \operatorname{argmax}_a Q_r^\pi(s, a). \quad (3)$$

The successor representation The *successor representation* (SR; (Dayan, 1993)) is motivated by the idea that an internal state representation for policy evaluation should be dependent on the similarity of different paths under the current policy. The SR is defined as an agent’s expected discounted state occupancy under a given policy, and for discrete state spaces can be stored in an $|\mathcal{S}| \times |\mathcal{S}|$ matrix M^π , where

$$M^\pi(s, s') := \mathbb{E}_\pi \left[\sum_k \gamma^k \mathbb{1}(s_{t+k} = s') \middle| s_t = s \right] = \mathbb{E}_\pi \left[\mathbb{1}(s_t = s') + \gamma M^\pi(s_{t+1}, s') \middle| s_t = s \right], \quad (4)$$

where $\mathbb{1}(\cdot)$ is an indicator function which evaluates to 1 when its argument is true and 0 otherwise. The SR can also be conditioned on actions, i.e., $M^\pi(s, a, s') := \mathbb{E}_\pi \left[\sum_k \gamma^k \mathbb{1}(s_{t+k} = s') \middle| s_t = s, a_t = a \right]$, and expressed in a vectorized format, we can write $M^\pi(s) := M^\pi(s, \cdot)$ or $M^\pi(s, a) := M^\pi(s, a, \cdot)$. The recursion in Eq. (4) admits a TD error:

$$\delta_t^M := \mathbf{1}(s_t) + \gamma M^\pi(s_{t+1}, \pi(s_{t+1})) - M^\pi(s_t, a_t), \quad (5)$$

where $\mathbf{1}(s_t)$ is a one-hot state representation of length $|\mathcal{S}|$. One useful property of the SR is that, once converged, it facilitates rapid policy evaluation for any reward function in a given environment:

$$\mathbf{r}^\top M^\pi(s, a) = \mathbf{r}^\top \mathbb{E}_\pi \left[\sum_k \gamma^k \mathbb{1}(s_{t+k}) \middle| s_t = s, a_t = a \right] = \mathbb{E}_\pi \left[\sum_k \gamma^k r_{t+k} \middle| s_t = s, a_t = a \right] = Q_r^\pi(s, a). \quad (6)$$

Fast transfer for multiple tasks In the real world, we often have to perform multiple tasks within a single environment. A simplified framework for this scenario is to consider a set of MDPs \mathcal{M} that share every property (i.e., $\mathcal{S}, \mathcal{A}, p, \gamma, \mu$) except reward functions, where each task within this family is determined by a reward function r belonging to a set \mathcal{R} . Extending the notions of policy evaluation and improvement to this multitask setting, we can define *generalized policy evaluation* (GPE) as the computation of the value function of a policy π on a set of tasks \mathcal{R} . Similarly, *generalized policy improvement* (GPI) for a set of “base” policies Π is the definition of a policy π' such that

$$Q_r^{\pi'}(s, a) \geq \sup_{\pi \in \Pi} Q_r^\pi(s, a) \quad \forall (s, a) \in \mathcal{S} \times \mathcal{A} \quad (7)$$

for some $r \in \mathcal{R}$. Naïvely, performing GPE requires $|\Pi|$ runs of a generic policy evaluation algorithm. How can an agent take advantage of the shared structure among the tasks in \mathcal{M} ? As hinted above, the SR offers a solution by decoupling the agent’s evaluation of its expected transition dynamics under a given policy from a specific reward function. Then, rather than needing to directly estimate $Q^\pi \forall \pi \in \Pi$, M^π only needs to be computed once, and given a new reward vector \mathbf{r} , the agent can quickly perform GPE via Eq. (6). As shown by Barreto et al. (2017a), it’s then possible to combine GPE and GPI to define a new policy π' via

$$\pi'(s) \in \operatorname{argmax}_{a \in \mathcal{A}} \max_{\pi \in \Pi} \mathbf{r}^\top M^\pi(s, a). \quad (8)$$

For brevity, we will refer to this combined procedure of GPE and GPI simply as “GPI”, unless otherwise noted. The resulting policy π' is guaranteed to perform at least as well as any individual $\pi \in \Pi$ (Barreto et al., 2020) and is part of a larger class of policies termed *set-improving policies* which perform at least as well as any single policy in a given set (Zahavy et al., 2021).

3 The First-Occupancy Representation

While the SR encodes states via expected occupancy across an arbitrary horizon, this may not be ideal in all situations. If a task has no fixed time limit but terminates once the agent reaches a pre-defined goal state, or if reward in a given state is consumed or made otherwise unavailable once encountered, a more useful representation would instead measure the duration until a policy is expected to reach states the *first* time. This observation motivates the *first-occupancy representation* (FR).

Definition 3.1. For an MDP with finite \mathcal{S} , the first-occupancy representation (FR) for a policy π $F^\pi \in [0, 1]^{|\mathcal{S}| \times |\mathcal{S}|}$ is given by

$$F^\pi(s, s') := \mathbb{E}_\pi \left[\sum_{k=0}^{\infty} \gamma^k \mathbb{1}(s_{t+k} = s', s' \notin \{s_{t:t+k}\}) \middle| s_t \right], \quad (9)$$

where $\{s_{t:t+k}\} = \{s_t, s_{t+1}, \dots, s_{t+k-1}\}$, with the convention that $\{s_{t:t+0}\} = \emptyset$.

In other words, as the indicator function equals 1 iff $s_{t+k} = s'$ and time $t+k$ is the first occasion on which the agent has occupied s' since time t , $F^\pi(s, s')$ gives the expected discount at the time the policy first reaches s' starting from s . We can then derive a recursive relationship for the FR:

$$\begin{aligned} F^\pi(s, s') &= \mathbb{E}_\pi \left[\mathbb{1}(s_t = s', s' \notin \emptyset) + \sum_{k=1}^{\infty} \gamma^k \mathbb{1}(s_{t+k} = s', s' \notin \{s_{t:t+k}\}) \middle| s_t \right] \\ &= \mathbb{E}_\pi \left[\mathbb{1}(s_t = s') + \sum_{k=1}^{\infty} \gamma^k \mathbb{1}(s_{t+k} = s', s_t \neq s', s' \notin \{s_{t+1:t+k}\}) \middle| s_t \right] \\ &= \mathbb{E}_\pi \left[\mathbb{1}(s_t = s') + \gamma \mathbb{1}(s_t \neq s') F^\pi(s_{t+1}, s') \middle| s_t \right] \\ &= \mathbb{1}(s_t = s') + \gamma \mathbb{1}(s_t \neq s') \mathbb{E}_{s_{t+1} \sim p^\pi(\cdot|s)} [F^\pi(s_{t+1}, s')] \end{aligned} \quad (10)$$

This recursion implies the following Bellman operator, analogous to the one used for policy evaluation:

Definition 3.2 (FR Operator). Let $F \in \mathbb{R}^{|\mathcal{S}| \times |\mathcal{S}|}$ be an arbitrary real-valued matrix. Then let \mathcal{G}^π denote the Bellman operator for the FR, such that

$$\mathcal{G}^\pi F = I_{|\mathcal{S}|} + \gamma(\mathbf{1}\mathbf{1}^\top - I_{|\mathcal{S}|})P^\pi F, \quad (11)$$

where $\mathbf{1}$ is the length- $|\mathcal{S}|$ vector of all ones. In particular, for a stationary policy π , $\mathcal{G}^\pi F^\pi = F^\pi$.

The following result establishes \mathcal{G}^π as a contraction, with the proof provided in Appendix A.3.

Proposition 3.1 (Contraction). Let \mathcal{G}^π be the operator as defined in Definition 3.2 for some stationary policy π . Then for any two matrices $F, F' \in \mathbb{R}^{|\mathcal{S}| \times |\mathcal{S}|}$,

$$|\mathcal{G}^\pi F(s, s') - \mathcal{G}^\pi F'(s, s')| \leq \gamma |F(s, s') - F'(s, s')|, \quad (12)$$

with the difference equal to zero for $s = s'$.

This implies the following convergence property of \mathcal{G}^π .

Proposition 3.2 (Convergence). Under the conditions assumed above, set $F^{(0)} = I_{|\mathcal{S}|}$. For $k = 0, 1, \dots$, suppose $F^{(k+1)} = \mathcal{G}^\pi F^{(k)}$. Then

$$|F^{(k)}(s, s') - F^\pi(s, s')| < \gamma^k \quad (13)$$

for $s \neq s'$ with the difference for $s = s'$ equal to zero $\forall k$.

Proof. We have, for $s \neq s'$ and using the notation $X_{s,s'} = X(s, s')$ for a matrix X ,

$$\begin{aligned} |(F^{(k)} - F^\pi)_{s,s'}| &= |(\mathcal{G}^k F^{(0)} - \mathcal{G}^k F^\pi)_{s,s'}| \\ &\leq \gamma^k |(F^{(0)} - F^\pi)_{s,s'}| \quad (\text{Proposition 3.1}) \\ &= \gamma^k F^\pi(s, s') < \gamma^k \quad (F^\pi(s, s') \in [0, 1)). \end{aligned} \quad (14)$$

For $s = s'$, $|(F^{(k)} - F^\pi)_{s,s}| = |1 - 1| = 0 \forall k$. □

Therefore, repeated applications of the FR Bellman operator $\mathcal{G}^k F \rightarrow F^\pi$ as $k \rightarrow \infty$. When the transition matrix P^π is unknown, the FR can instead be updated through the following TD error:

$$\delta_t^F = \mathbb{1}(s_t = s') + \gamma(1 - \mathbb{1}(s_t = s'))F^\pi(s_{t+1}, s') - F^\pi(s_t, s'). \quad (15)$$

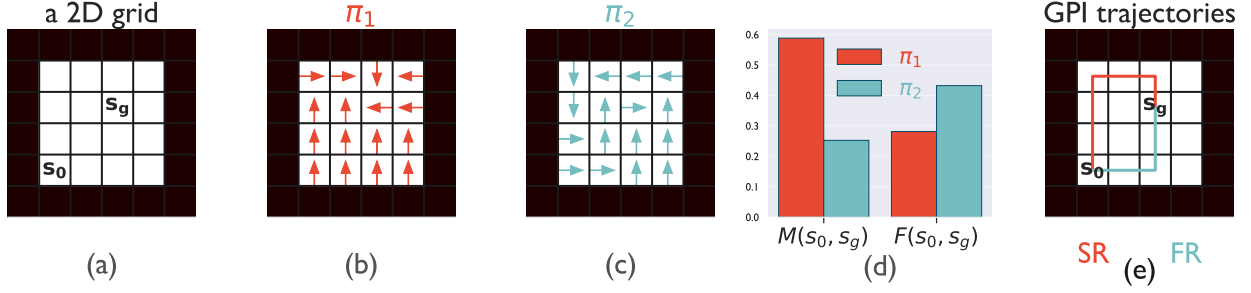


Figure 1: **The FR is higher for shorter paths between states.** (a) A 2D gridworld with fixed start state s_0 and reward state s_g . (b-c) π_1 takes longer to reach s_g , but revisits it infinitely often. π_2 reaches s_g more quickly, but never returns. (d) The FR from s_0 to s_g is higher for π_2 , but the corresponding SR is lower. (e) Due to this difference, GPI with the SR will select π_1 , while GPI with the FR selects π_2

In all experiments throughout the paper, the FR is learned via TD updates, rather than via dynamic programming.

To gain intuition for the FR, we can imagine a 2D environment with a fixed start state s_0 , a single rewarded state s_g , and deterministic transitions (Fig. 1a). One policy, π_1 , reaches s_g slowly, but after encountering it for the first time, re-enters s_g infinitely often (Fig. 1b). A second policy, π_2 , reaches s_g quickly but never occupies it again (Fig. 1c). In this setting, because π_1 re-enters s_g multiple times, despite arriving there more slowly than π_2 , $M^{\pi_1}(s_0, s_g) > M^{\pi_2}(s_0, s_g)$, but because the FR only counts the first occupancy of a given state, $F^{\pi_1}(s_0, s_g) < F^{\pi_2}(s_0, s_g)$. In this way, the FR reflects the path length between states under a given policy. Interestingly, like the SR, the FR can also be used to encourage exploration.

The FR as an Exploration Bonus In Machado et al. (2020), the SR is proposed as a useful representation to encourage exploration in tasks with sparse or deceptive rewards. Specifically, they propose to use the norm of the SR as a bonus in on-policy learning with Sarsa (Rummery & Niranjan, 1994; Sutton & Barto, 2018):

$$\delta_t = r_t + \frac{\beta}{\|M^\pi(s_t)\|_1} + \gamma Q^\pi(s_{t+1}, \pi(s_{t+1})) - Q^\pi(s_t, a_t), \quad (16)$$

where $\beta \in \mathbb{R}$ controls the size of the exploration bonus and M^π is updated using Eq. (5). In the limit as $t \rightarrow \infty$, $\|M^\pi(s)\|_1 \rightarrow 1/(1-\gamma) \forall s$, but during learning, Machado et al. (2020) show that $\|M^\pi(s)\|_1$ can act as a proxy for the state-visit count $n(s)$, with $\|M^\pi(\cdot)\|_1^{-1}$ rewarding the agent the first time it visits a state and decreasing in magnitude for every subsequent visit. It’s important to observe, however, that concentrating in a few states will *reduce* the size of the bonus, not remove it. To encourage exploration, it makes sense to only reward the discovery of states that haven’t previously been encountered. In contrast to $\|M^\pi(s)\|_1$, which inevitably tends to $1/(1-\gamma)$, $\|F^\pi(s)\|_1 \leq \frac{1-\gamma^{|S|+1}}{1-\gamma}$, with equality for a given state only if the policy reaches every other state from that location. Because $\|F^\pi\|_1$ only grows when new states are discovered (or shorter paths to previously encountered states), we can instead augment Sarsa as follows:

$$\delta_t = r_t + \beta \|F^\pi(s_t)\|_1 + \gamma Q^\pi(s_{t+1}, \pi(s_{t+1})) - Q^\pi(s_t, a_t). \quad (17)$$

We tested our approach empirically on the RiverSwim and SixArms environments (Strehl & Littman, 2008), two hard-exploration tasks from the PAC-MDP literature. In both tasks, visualized in Appendix Fig. 9, it’s very easy for the agent to obtain a small reward in a state that’s easy to reach by virtue of the environment transition dynamics, while much greater reward is available in harder to reach states. In both cases, we ran regular Sarsa, Sarsa with an SR bonus (Sarsa + SR) and SARSA with an FR bonus (Sarsa + FR) for 5,000 time steps, acting with an ϵ -greedy policy to maximize the discounted return. The results are listed in Table 1, where we can see that the FR results in an added benefit over the SR. We believe developing further understanding of these results and the relationship between the FR and the SR and exploration represents an interesting topic for future work.

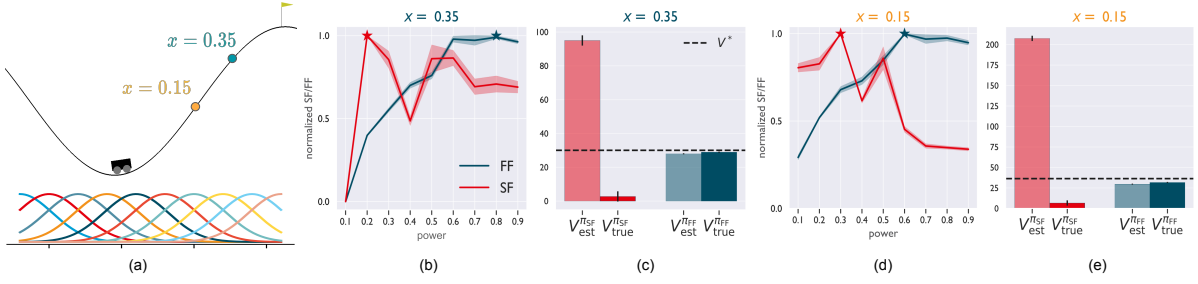


Figure 2: The FF facilitates accurate policy evaluation and selection.

Task	Sarsa + FR	Sarsa + SR	Sarsa
RiverSwim	1,547,243 \pm 340,501	1,197,075 \pm 369,991	25,075 \pm 12,247
SixArms	1,191,496 \pm 429,421	1,025,750 \pm 490,951	376,655 \pm 84,490

Table 1: Exploration task results. \pm values denote one standard deviation across 100 trials.

Policy evaluation and improvement with the FR Like the SR, we can quickly perform policy evaluation with the FR. Crucially, however, the FR induces the following value function:

$$\mathbf{r}^\top F^\pi(s, a) = \mathbf{r}^\top \mathbb{E}_\pi \left[\sum_k \gamma^k \mathbb{1}(s_{t+k}, s_{t:t+k}) \middle| s_t, a_t \right] = \mathbb{E}_\pi \left[\sum_k \gamma^k r_{t+k}^F \middle| s_t, a_t \right] := Q_{r^F}^\pi(s, a), \quad (18)$$

where $r^F : \mathcal{S} \rightarrow \mathbb{R}$ is a reward function such that $r^F(s_{t+k}) = r(s_{t+k})$ if $s_{t+k} \notin \{s_{t:t+k}\}$ and 0 otherwise. In other words, multiplying any reward vector by the FR results in the value function for a corresponding task with *non-Markovian* reward structure in which the agent obtains rewards from states only once. This is a very common feature of real-world tasks, such as foraging for food or reaching a target. Accordingly, there is a rich history of studying tasks with this kind of structure, termed *non-Markovian reward decision processes* (NMRDPs; (Bacchus et al., 1996; Peshkin et al., 2001; Littman et al., 2017; Gaon & Brafman, 2020)). Helpfully, all NMRDPs can be converted into an equivalent MDP with an appropriate transformation of the state space (Bacchus et al., 1996). For example, if reward depends on whether the agent has picked up a particular kind of object and brought it to a specific location, but the native state space does not represent whether the object has been picked up, adding a single bit to the state representation indicating the condition of the object is sufficient to make the problem Markovian (Peshkin et al., 2001).

Most approaches in this family attempt to be generalists, *learning* an appropriate state transformation and encoding it using some form of logical calculus or finite state automaton (Bacchus et al., 1996; Littman et al., 2017; Gaon & Brafman, 2020). While it would technically be possible to learn or construct the transformation required to account for the non-Markovian nature of r^F , it would be exponentially expensive in $|\mathcal{S}|$, as every path would need to account for the first occupancy of each state along the path. That is, $|\mathcal{S}|$ bits would need to be added to each successive state in the trajectory. Crucially, the FR has the added advantage of being task-agnostic, in that for *any* reward function r in a given environment, the FR can immediately perform policy evaluation for the corresponding r^F .

Infinite state spaces A natural question when extending the FR to real-world scenarios is how it can be generalized to settings where $|\mathcal{S}|$ is either impractically large or infinite. In these cases, the SR is reframed as *successor features* ψ^π (SFs; (Kulkarni et al., 2016; Barreto et al., 2017b)), where the d th SF is defined as follows:

$$\psi_d^\pi(s) := \mathbb{E}_\pi \left[\sum_{k=0}^{\infty} \gamma^k \phi_d(s_{t+k}) \middle| s_t = s \right], \quad (19)$$

where $d = 1, \dots, D$ and $\phi : \mathcal{S} \rightarrow \mathbb{R}^D$ is a *base feature* function. The base features $\phi(\cdot)$ are typically defined so that a linear combination predicts immediate reward (i.e., $\mathbf{w}^\top \phi(s) = r(s)$ for some $\mathbf{w} \in \mathbb{R}^D$), and there are a number of approaches to learning them (Kulkarni et al., 2016; Barreto et al., 2018; Ma et al., 2020). A

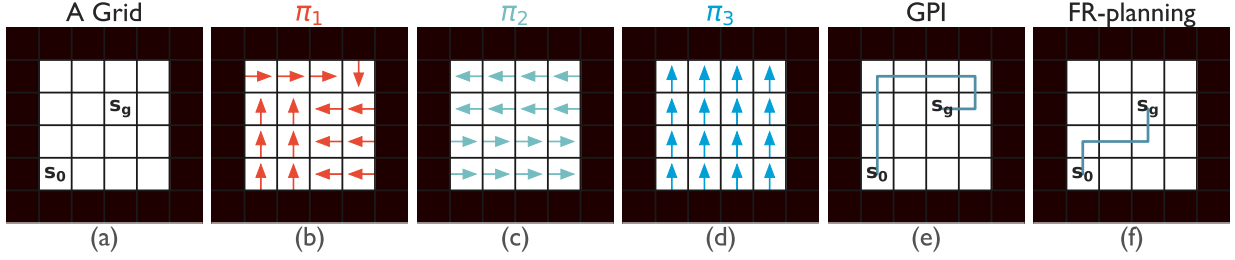


Figure 3: **The FR enables efficient planning.** (a) A 2D gridworld with fixed start state s_0 and reward state s_g . (b-d) π_1 takes a long path to reach s_g , but is the only policy to reach s_g on its own. Neither π_2 nor π_3 reach s_g on their own, but can be stitched together to reach s_g more quickly than π_1 . (e) GPI follows π_1 . (f) Planning with the FR enables the construction of a shorter path.

natural extension to continuous \mathcal{S} for the FR would be to define a *first-occupancy feature* (FF) representation φ^π , where the d th FF is given by

$$\varphi_d^\pi(s) := \mathbb{E}_\pi \left[\sum_{k=0}^{\infty} \gamma^k \mathbb{1}(\phi_d(s_{t+k}) \geq \theta_d, \{\phi_d(s_{t'})\}_{t'=t:t+k} < \theta_d) \middle| s_t = s \right] \quad (20)$$

$$= \mathbb{1}(\phi_d(s_t) \geq \theta_d) + \gamma(1 - \mathbb{1}(\phi_d(s_t) \geq \theta_d)) \mathbb{E}_{s_{t+1} \sim p^\pi} [\varphi_d^\pi(s_{t+1})] \quad (21)$$

where θ_d is a threshold value for the d th feature. The indicator then evaluates to one only if $\phi_d(s_{t+k})$ is the first state from time t to $t+k$ whose feature embedding exceeds the threshold. Note that this representation recovers the FR when the feature function is a one-hot state encoding and the thresholds $\{\theta_d\}_{d=1}^D$ are all 1.

We demonstrate the usefulness of this representation in the unsupervised pre-training RL (URL) setting, a paradigm which has gained popularity recently as a possible solution to the high sample complexity of deep RL algorithms (Liu & Abbeel, 2021; Gregor et al., 2016; Eysenbach et al., 2018; Sharma et al., 2020). In URL, the agent first explores an environment without extrinsic reward before being exposed to a test task. The objective of the exploration period is to gain an understanding (learn a representation) of the environment which can be leveraged for efficient adaptation to new goals. Here, we use a simple environment, a modified version of the continuous MountainCar task from OpenAI Gym (Brockman et al., 2016). In our set-up, which we repeated for 20 random seeds, (Fig. 2(a), further details in Appendix A.2), the agent is given a pre-training period of 20,000 timesteps in a rewardless environment, during which it learns FFs or SFs for a set of policies Π which swing back and forth in the environment with a fixed acceleration or “power” (pseudo-code provided in Appendix A.2). The goal of the agent during the testing phase is to identify the policy $\pi \in \Pi$ which reaches a randomly sampled terminal goal location as quickly as possible. We use radial basis functions as the base features $\phi_d(\cdot)$ (shown in Fig. 2(a)) with fixed thresholds $\theta_d = 0.7 \forall d$ for the FFs.

Fig. 2(b) plots the FF and SF values versus policy power from the start state for two different goal locations. The low-power policies require more time to gain momentum up the hill, but the policies which maximize the SF values slow down around the goal locations, dramatically increasing their total “occupancy” of that area. In contrast, high-powered policies reach the goal locations for the first time much sooner, and so the policies with the highest FF values have higher powers. In the test phase, the agent fits the reward vector $\mathbf{w} \in \mathbb{R}^D$ by minimizing $\sum_t \|r_t - \mathbf{w}^\top \phi(s_t)\|^2$, as is standard in the SF literature (Barreto et al., 2017b;a; 2018; 2020; Zahavy et al., 2021). The agent then follows the set-max policy (SMP; (Zahavy et al., 2021)), which selects the policy in Π which has the highest expected value across starting states: $\pi^{\text{SMP}} \in \arg\max_{\pi \in \Pi} \mathbb{E}_{s_0 \sim \mu} [V^\pi(s_0)]$, where $V^\pi(s_0) = \mathbf{w}^\top \varphi^\pi(s_0)$ (with φ^π replaced by ψ^π for SF-based value estimates). Fig. 2(c) shows both the estimated (V_{est}) and true (V_{true}) values of the SMPs selected using both the SF and FF, along with the value of the optimal policy V^* . We can see that the accumulation of the SFs results in a significant overestimation in value, as well as a suboptimal policy. The FF estimates are nearly matched to the true values of the selected policies for each goal location and achieve nearly optimal performance. This demonstrates the potential of the FF for further application in settings which require function approximation.

4 Implicit Planning with the FR

While GPI is a fast and effective method for composing previously learned policies to perform well on new tasks, it is limited in that it is only able to select actions based on a one-step lookahead in the environment,

which may cause it to behave suboptimally. One simple situation that highlights such a scenario is depicted in Fig. 3. As before, there are start and goal states in a simple room (Fig. 3(a)), but here there are three policies comprising the set $\Pi = \{\pi_1, \pi_2, \pi_3\}$ (Fig. 3(b-d)). GPI selects π_1 because it is the only policy that reaches the goal s_g within one step of the start s_0 : $\pi_1 = \max_{\pi \in \Pi} \mathbf{r}^\top M^\pi(s_0, s_g)$ (Fig. 3(e)). (Note that using GPI with the FR instead would also lead to this choice.) To gain further intuition for the FR versus the SR, we can visualize the representations for the policies in Fig. 3. However, the optimal strategy using the policies in Π is instead to move right using π_2 and up using π_3 . How can the FR be used to find such a sequence?

Intuitively, starting in a state s , this type of strategy is grounded in following one policy until a certain state s' and then *switching* to a different policy in the base set. Because the FR effectively encodes the shortest path between each pair of states (s, s') for a given policy, the agent can elect to follow the policy $\pi \in \Pi$ with the greatest value of $F^\pi(s, s')$, then switch to another policy and repeat the process until reaching a desired state. If the target state is known to the agent, this process of selecting policies and intermediate states at which to switch can be completed before acting and thought of as forming a *plan*, with the switching states serving as *subgoals*. Note that our use of the word plan here differs from the classical term “planning” in MB RL. The resulting approach is in fact more closely related to the hierarchical *options* framework (Sutton et al., 1999; Sutton & Barto, 2018), with the critical difference being the transferrability of the underlying representations, which enable optimal path-planning across multiple MDPs. For a more detailed discussion, see Appendix A.6.

More formally, we can construct a DP algorithm to solve for the optimal sequence of planning policies π^F and subgoals s^F . Denoting by $\Gamma_k(s)$ the total discount of the full trajectory from s to s_g at step k of the procedure, we jointly optimize over policies π and subgoals s' for each state s :

$$\begin{aligned} \Gamma_{k+1}(s) &= \max_{\pi \in \Pi, s' \in \mathcal{S}} F^\pi(s, s') \Gamma_k(s') \\ \pi_{k+1}^F(s), s_{k+1}^F(s) &= \operatorname{argmax}_{\pi \in \Pi, s' \in \mathcal{S}} F^\pi(s, s') \Gamma_k(s'). \end{aligned} \quad (22)$$

Intuitively, the product $F^\pi(s, s') \Gamma_k(s')$ can be interpreted as the expected discount of the plan consisting of following π from s to s' , then the current best (shortest-path) plan from s' to s_g . The full procedure, which we refer to as FR-planning (FRP), is given in Alg. 1. Fig. 5 depicts the resulting policies π^F and subgoals s^F obtained from running FRP on the example in Fig. 3. Importantly, an agent equipped with π^F and s^F can either construct an explicit plan as a sequence of $(\pi^F(s), s^F(s))$ tuples which determine which policy to use in a given state and where to switch to the next policy (for detail, see Alg. 2), or it can simply follow $\pi^F(s)$ in each state, where π^F can be seen as forming an *implicit* plan.

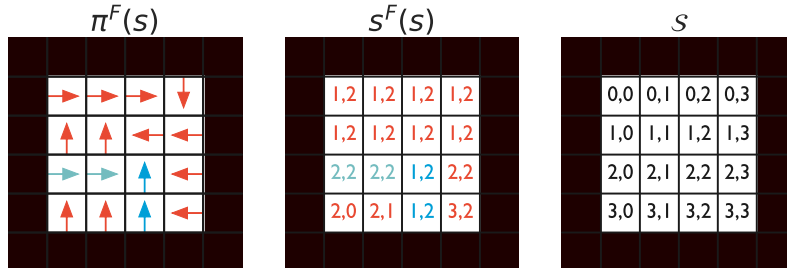


Figure 5: **Implicit planning output.** (Left) The planning policies $\pi^F(s)$ that the agent will elect to follow in each state en route to the goal (see Fig. 3(a)). Arrows denote the action taken by the chosen policy in each state. (Middle) The (row, column) subgoals for each state $s^F(s)$. (Right) The state space \mathcal{S} , for reference.

We can see that running an agent equipped with the plan shown in Fig. 5 does indeed find a shortest path to s_g (Fig. 3(e)). The following result shows that under certain assumptions, FRP provably finds the shortest path to a given goal location, with the proof provided in Appendix A.3.

Algorithm 1: FR Planning

```

1: input: goal state  $s_g$ , base policies  $\Pi = \{\pi_1, \dots, \pi_n\}$  and FRs  $\{F^{\pi_1}, \dots, F^{\pi_n}\}$ .
2: // initialize discounts-to-goal  $\Gamma$ 
3:  $\Gamma_0(s) \leftarrow -\infty \forall s \in \mathcal{S}$ 
4: for  $s \in \mathcal{S}$  do
5:    $\Gamma_1(s) \leftarrow \max_{\pi \in \Pi} F^\pi(s, s_g)$ 
6:    $\pi_1^F(s) \leftarrow \operatorname{argmax}_{\pi \in \Pi} F^\pi(s, s_g)$ 
7:    $s_1^F(s) \leftarrow s_g$ 
8: end for
9: // iteratively refine  $\Gamma$ 
10:  $k \leftarrow 1$ 
11: while  $\exists s \in \mathcal{S}$  such that  $\Gamma_k(s) > \Gamma_{k-1}(s)$  do
12:   for  $s \in \mathcal{S}$  do
13:      $\Gamma_{k+1}(s) \leftarrow \max_{\pi \in \Pi, s' \in \mathcal{S}} F^\pi(s, s') \Gamma_k(s')$ 
14:      $\pi_{k+1}^F(s), s_{k+1}^F(s) \leftarrow \operatorname{argmax}_{\pi \in \Pi, s' \in \mathcal{S}} F^\pi(s, s') \Gamma_k(s')$ 
15:   end for
16:    $k \leftarrow k + 1$ 
17: end while
18: return  $\pi^F, s^F$ 

```

Proposition 4.1 (Planning optimality). *Consider a finite MDP with deterministic transitions, a single goal state s_g , and a base policy set Π composed of deterministic policies $\pi : \mathcal{S} \rightarrow \mathcal{A}$, $\forall \pi \in \Pi$. We make the following coverage assumption: there exists some sequence of policies that reaches s_g from a given start state s_0 . Under these conditions, Alg. 1 converges such that $\Gamma^\Pi(s_0) = \gamma^{L_\Pi^*}$, where L_Π^* is the shortest path length from s_0 to s_g using $\pi \in \Pi$.*

Performance and computational cost We can see that each iteration of the planning algorithm adds at most one new subgoal to the planned trajectory from each state to the goal, with convergence when no policy switches can be made that reduce the number of steps required. If there are K iterations, the overall computational complexity of FRP is $\mathcal{O}(K|\Pi||\mathcal{S}|^2)$. In contrast, running value iteration (VI; (Sutton & Barto, 2018)) for N iterations is $\mathcal{O}(N|\mathcal{A}||\mathcal{S}|^2)$. Given the true transition matrix P and reward vector \mathbf{r} , VI will also converge to the shortest path to a specified goal state; but FRP converges more quickly than VI whenever $K|\Pi| < N|\mathcal{A}|$. To achieve an error ϵ between the estimated value function and the value function of the optimal policy, VI requires $N \geq \frac{1}{(1-\gamma)} \log \frac{2}{(1-\gamma)^2 \epsilon}$ (Puterman, 1994), which for $\gamma = 0.95$ and $\epsilon = 0.1$ (as an example), gives $N \geq 180$ iterations¹. To test convergence rates in practice, we applied FRP, VI, and GPI using the FR to the classic FourRoom environment (Sutton et al., 1999) on a modified task in which agents start in the bottom left corner and move to a randomly located goal state. Once the goal is reached, a new goal is randomly sampled in a different location until the episode is terminated after 75 timesteps. For GPI and FRP, we use four base policies which each only take one action: {up, down, left, right}. We ran each algorithm for 100 episodes, with the results plotted in Fig. 6(a). Note that here GPI is equivalent to FRP with $K = 0$ iterations. To see this, observe that when there is a single goal s_g such that only $r(s_g) > 0$, the policy selected by GPI is

$$\pi^{\text{GPI}}(s) \in \operatorname{argmax}_{\pi \in \Pi} \mathbf{r}^\top F^\pi(s) = \operatorname{argmax}_{\pi \in \Pi} r(s_g) F^\pi(s, s_g) = \operatorname{argmax}_{\pi \in \Pi} F^\pi(s, s_g). \quad (23)$$

Therefore, GPI selects the policy for which $F^\pi(s, s_g)$ is the highest, just as FRP does for $K = 0$. When there are n goal states with equal reward, finding the ordering of the goals that results in the shortest expected path involves a simple procedure, but is in general $\mathcal{O}(n!)$ (see Appendix A.5 for a discussion). Due to the nature of the base policies in the above case, the number of subgoals on any given path is equal to the number of turns the agent must take from its current state to the current goal, which for this environment is three. We can then see that FRP reaches the optimal performance obtained by the converged VI after $K = 3$ iterations (Fig. 6(a)). In contrast, for the same number of iterations, VI performs far worse. The trajectories between goals taken by FRP for $K = 0$ and $K = 3$ iterations are plotted in Fig. 6(b) for an example episode.

¹Other DP methods like policy iteration (PI), which is strongly polynomial, converge more quickly than VI, but in the example above, PI still needs $N \geq \log(1/((1-\gamma)\epsilon))/(1-\gamma) = 106$ (Ye, 2011), for instance.

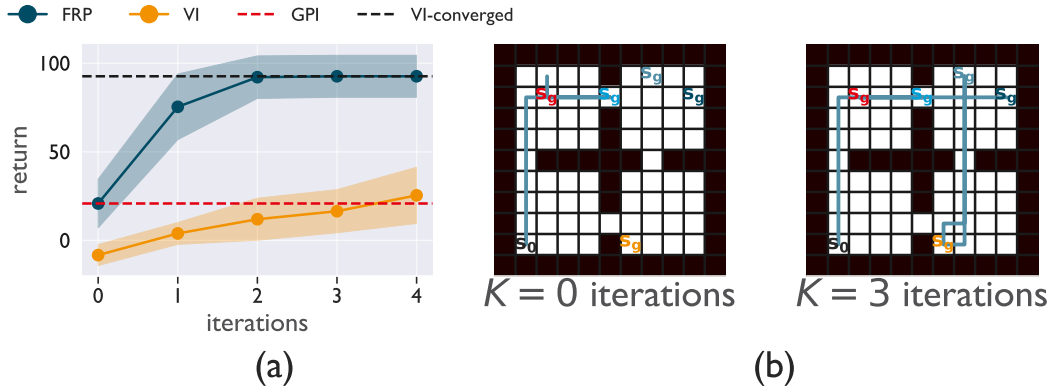


Figure 6: **Implicit planning interpolates between GPI and model-based DP.** Error shading represents one standard deviation and is omitted for clarity for GPI and VI-converged

Stochastic environments While we currently lack theoretical guarantees for stochastic environments, we empirically tested FRP on the above FourRoom task with added transition noise ϵ . That is, the agent moves to a random adjacent state with probability ϵ regardless of action. We compared FRP to VI run to convergence for increasing ϵ , with the results plotted in Fig. 7. FRP is able to match the performance of VI at every level of noise, indicating a strong robustness to stochasticity in practice.

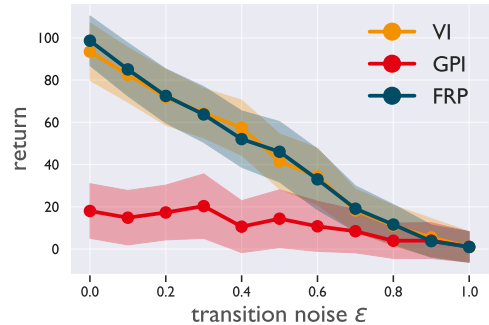


Figure 7: **Implicit planning succeeds even with noisy transitions.** Error shading denotes one standard deviation.

4.1 Escape Behavior

In prey species such as mice, escaping from threats using efficient paths to shelter is critical for survival (Lima & Dill, 1990). Recent work studying the strategies employed by mice when fleeing threatening stimuli in an arena containing a barrier has indicated that, rather than use an explicit cognitive map, mice instead appear to memorize a sequence of subgoals to plan efficient routes to shelter (Shamash et al., 2021). When first exposed to threat, some animals ran along a direct homing path and thus encountered the barrier. Over subsequent identical trials spanning 20 minutes of exploration, threat-stimulus presentation, and escape, mice learned to navigate directly to the edge of the wall before switching direction towards the shelter (Fig. 8). Follow-up control experiments suggest that mice acquire persistent spatial memories of subgoal locations for efficient escapes. Here, we design a task in which planning using the FR induces behavior that is consistent with these experiments.

We model the initial escape trial by an agent with a partially learned FR, leading to a suboptimal escape plan leading directly to the barrier. Upon hitting the barrier, sensory input prompts rapid re-planning to navigate around the obstacle. The FR is then updated and the escape plan is recomputed, simulating subsequent periods of exploration during which the mouse presumably memorizes subgoals. We find a similar pattern of behavior to that of mice (Fig. 8(b)). See Appendix A.2 for experimental details.

We do not have evidence, nor do we claim, that this is the exact process by which mice are able to efficiently learn escape behavior. Rather, we demonstrate that the FR facilitates behavior that is consistent with our understanding of animal learning in tasks which demand efficient planning. Given the recent evidence in support of SR-like representations in the brain (Stachenfeld et al., 2017; Momennejad et al., 2017), we are optimistic about the possibility of neural encodings of FR-like representations as well.

5 Conclusion

In this work, we have introduced the first-occupancy representation, a compiled model which encodes the expected discount associated with transitions between states for a given policy. We explored its basic properties, including its compatibility with standard RL techniques such as learning through bootstrapping

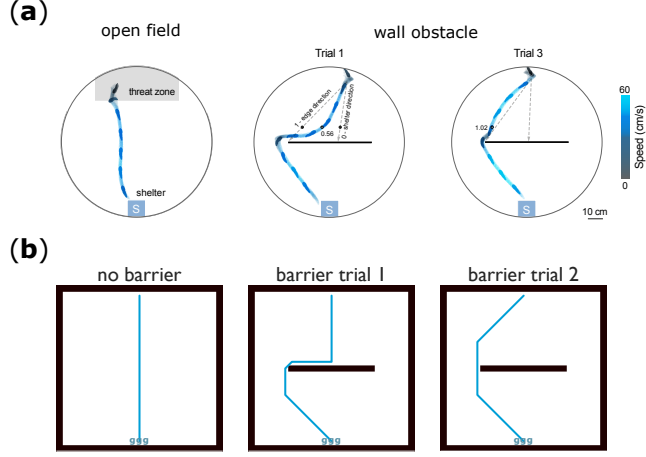


Figure 8: **The FR induces biologically-realistic behavior.**

and sampled experience, as well as its support for learning in environments with an ethologically important type of non-Markovian reward structure. We then demonstrated that the FR supports a form of efficient planning, which in certain settings results in provably optimal trajectories, and that this approach induces similar behavioral strategies to those observed in mice escaping from perceived threats.

As with any new approach, there are limitations. However, we believe that these limitations represent opportunities for future work. From a theoretical perspective, it will be important to more precisely characterize the behavior of FRP in stochastic environments. For generalizing the FR to continuous state spaces, it will be necessary to more fully explore and develop understanding of the first-feature representation. In particular, FRP is naturally restricted to discrete state spaces. A more natural extension would be to *partially-observable* MDPs with continuous observation spaces and discrete latent states (e.g., (Vértes & Sahani, 2019; Du et al., 2019)). Finally, it would be informative to test hypotheses of FR-like representations in the brain through neural data analysis. We hope this research direction will inspire advancements on representations that can support efficient behavior in realistic settings.

References

- Mohammad Gheshlaghi Azar, Rémi Munos, and Hilbert J. Kappen. Minimax pac bounds on the sample complexity of reinforcement learning with a generative model. *Machine Learning*, 91(3):325–349, 2013. URL <https://doi.org/10.1007/s10994-013-5368-1>.
- Fahiem Bacchus, Craig Boutilier, and Adam Grove. Rewarding behaviors. In *Proceedings of the Thirteenth National Conference on Artificial Intelligence - Volume 2*, AAAI’96, pp. 1160–1167. AAAI Press, 1996.
- Andre Barreto, Will Dabney, Remi Munos, Jonathan J Hunt, Tom Schaul, Hado P van Hasselt, and David Silver. Successor features for transfer in reinforcement learning. In I. Guyon, U. V. Luxburg, S. Bengio, H. Wallach, R. Fergus, S. Vishwanathan, and R. Garnett (eds.), *Advances in Neural Information Processing Systems*, volume 30. Curran Associates, Inc., 2017a. URL <https://proceedings.neurips.cc/paper/2017/file/350db081a661525235354dd3e19b8c05-Paper.pdf>.
- Andre Barreto, Will Dabney, Remi Munos, Jonathan J Hunt, Tom Schaul, Hado P van Hasselt, and David Silver. Successor features for transfer in reinforcement learning. In I. Guyon, U. V. Luxburg, S. Bengio, H. Wallach, R. Fergus, S. Vishwanathan, and R. Garnett (eds.), *Advances in Neural Information Processing Systems*, volume 30. Curran Associates, Inc., 2017b. URL <https://proceedings.neurips.cc/paper/2017/file/350db081a661525235354dd3e19b8c05-Paper.pdf>.
- Andre Barreto, Diana Borsa, John Quan, Tom Schaul, David Silver, Matteo Hessel, Daniel Mankowitz, Augustin Zidek, and Remi Munos. Transfer in deep reinforcement learning using successor features and generalised policy improvement. In Jennifer Dy and Andreas Krause (eds.), *Proceedings of the 35th International Conference on Machine Learning*, volume 80 of *Proceedings of Machine Learning Research*, pp. 501–510. PMLR, 10–15 Jul 2018. URL <http://proceedings.mlr.press/v80/barreto18a.html>.
- Andre Barreto, Shaobo Hou, Diana Borsa, David Silver, and Doina Precup. Fast reinforcement learning with generalized policy updates. *Proceedings of the National Academy of Sciences*, 117(48):30079–30087, 2020. ISSN 0027-8424. doi: 10.1073/pnas.1907370117. URL <https://www.pnas.org/content/117/48/30079>.
- Timothy E.J. Behrens, Timothy H. Muller, James C.R. Whittington, Shirley Mark, Alon B. Baram, Kimberly L. Stachenfeld, and Zeb Kurth-Nelson. What is a cognitive map? organizing knowledge for flexible behavior. *Neuron*, 100(2):490–509, 2018. doi: <https://doi.org/10.1016/j.neuron.2018.10.002>. URL <https://www.sciencedirect.com/science/article/pii/S0896627318308560>.
- Richard Bellman. *Dynamic Programming*. Dover Publications, 1957.
- Greg Brockman, Vicki Cheung, Ludwig Pettersson, Jonas Schneider, John Schulman, Jie Tang, and Wojciech Zaremba. Openai gym, 2016.
- Peter Dayan. Improving generalization for temporal difference learning: The successor representation. *Neural Computation*, 5(4):613–624, 1993. doi: 10.1162/neco.1993.5.4.613.
- Simon S. Du, Akshay Krishnamurthy, Nan Jiang, Alekh Agarwal, Miroslav Dudík, and John Langford. Provably efficient rl with rich observations via latent state decoding, 2019.
- Benjamin Eysenbach, Abhishek Gupta, Julian Ibarz, and Sergey Levine. Diversity is all you need: Learning skills without a reward function, 2018.
- Maor Gaon and Ronen Brafman. Reinforcement learning with non-markovian rewards. *Proceedings of the AAAI Conference on Artificial Intelligence*, 34(04):3980–3987, Apr. 2020. doi: 10.1609/aaai.v34i04.5814. URL <https://ojs.aaai.org/index.php/AAAI/article/view/5814>.
- Samuel J. Gershman. The successor representation: Its computational logic and neural substrates. *Journal of Neuroscience*, 38(33):7193–7200, 2018. doi: 10.1523/JNEUROSCI.0151-18.2018. URL <https://www.jneurosci.org/content/38/33/7193>.
- Karol Gregor, Danilo Jimenez Rezende, and Daan Wierstra. Variational intrinsic control, 2016.
- Tejas D. Kulkarni, Ardavan Saeedi, Simanta Gautam, and Samuel J. Gershman. Deep successor reinforcement learning, 2016.
- Steven Lima and Larry Dill. Behavioral decisions made under the risk of predation: A review and prospectus. *Canadian Journal of Zoology-revue Canadienne De Zoologie - CAN J ZOOL*, 68:619–640, 04 1990. doi: 10.1139/z90-092.

- Michael L. Littman, Ufuk Topcu, Jie Fu, Charles Isbell, Min Wen, and James MacGlashan. Environment-Independent Task Specifications via GLTL. *arXiv e-prints*, 2017.
- Hao Liu and Pieter Abbeel. Aps: Active pretraining with successor features. In Marina Meila and Tong Zhang (eds.), *Proceedings of the 38th International Conference on Machine Learning*, volume 139 of *Proceedings of Machine Learning Research*, pp. 6736–6747. PMLR, 18–24 Jul 2021. URL <https://proceedings.mlr.press/v139/liu21b.html>.
- Chen Ma, Dylan R. Ashley, Junfeng Wen, and Yoshua Bengio. Universal successor features for transfer reinforcement learning, 2020.
- Marlos C. Machado, Marc G. Bellemare, and Michael Bowling. Count-based exploration with the successor representation. *Proceedings of the AAAI Conference on Artificial Intelligence*, 34(04):5125–5133, Apr. 2020. doi: 10.1609/aaai.v34i04.5955. URL <https://ojs.aaai.org/index.php/AAAI/article/view/5955>.
- Tamas Madarasz and Tim Behrens. Better transfer learning with inferred successor maps. In H. Wallach, H. Larochelle, A. Beygelzimer, F. d'Alché-Buc, E. Fox, and R. Garnett (eds.), *Advances in Neural Information Processing Systems*, volume 32. Curran Associates, Inc., 2019. URL <https://proceedings.neurips.cc/paper/2019/file/274a10ffa06e434f2a94df765cac6bf4-Paper.pdf>.
- I. Momennejad, E. M. Russek, J. H. Cheong, M. M. Botvinick, N. D. Daw, and S. J. Gershman. The successor representation in human reinforcement learning. *Nature Human Behaviour*, 1(9):680–692, 2017.
- Leonid Peshkin, Nicolas Meuleau, and Leslie Pack Kaelbling. Learning policies with external memory, 2001.
- Martin L Puterman. *Markov decision processes: discrete stochastic dynamic programming*. John Wiley & Sons, 1994.
- Martin L. Puterman. *Markov decision processes: discrete stochastic dynamic programming*. John Wiley and Sons, 2010.
- G. Rummery and Mahesan Niranjana. On-line q-learning using connectionist systems. *Technical Report CUED/F-INFENG/TR 166*, 11 1994.
- Philip Shamash, Sarah F. Olesen, Panagiota Iordanidou, Dario Campagner, Banerjee Nabhojit, and Tiago Branco. Mice learn multi-step routes by memorizing subgoal locations. *bioRxiv*, 2021. doi: 10.1101/2020.08.19.256867. URL <https://www.biorxiv.org/content/early/2021/05/08/2020.08.19.256867>.
- Archit Sharma, Shixiang Gu, Sergey Levine, Vikash Kumar, and Karol Hausman. Dynamics-aware unsupervised discovery of skills. In *International Conference on Learning Representations*, 2020. URL <https://openreview.net/forum?id=HJgLR4KvH>.
- David Silver and Kamil Ciosek. Compositional planning using optimal option models, 2012.
- Kimberly L Stachenfeld, Matthew M Botvinick, and Samuel J Gershman. The hippocampus as a predictive map. *Nature Neuroscience*, 20(11):1643–1653, 2017. URL <https://doi.org/10.1038/nn.4650>.
- Alexander L. Strehl and Michael L. Littman. An analysis of model-based interval estimation for markov decision processes. *Journal of Computer and System Sciences*, 74(8):1309–1331, 2008. ISSN 0022-0000. doi: <https://doi.org/10.1016/j.jcss.2007.08.009>. URL <https://www.sciencedirect.com/science/article/pii/S0022000008000767>. Learning Theory 2005.
- Richard S. Sutton and Andrew G. Barto. *Reinforcement Learning: An Introduction*. The MIT Press, second edition, 2018. URL <http://incompleteideas.net/book/the-book-2nd.html>.
- Richard S. Sutton, Doina Precup, and Satinder Singh. Between mdps and semi-mdps: A framework for temporal abstraction in reinforcement learning. *Artificial Intelligence*, 112(1):181–211, 1999. URL <https://www.sciencedirect.com/science/article/pii/S0004370299000521>.
- Eszter Vértés and Maneesh Sahani. A neurally plausible model learns successor representations in partially observable environments. In H. Wallach, H. Larochelle, A. Beygelzimer, F. d'Alché Buc, E. Fox, and R. Garnett (eds.), *Advances in Neural Information Processing Systems*, volume 32. Curran Associates, Inc., 2019. URL <https://proceedings.neurips.cc/paper/2019/file/dea184826614d3f4c608731389ed0c74-Paper.pdf>.

- Yinyu Ye. The simplex and policy-iteration methods are strongly polynomial for the markov decision problem with a fixed discount rate. *Mathematics of Operations Research*, 36(4):593–603, 2011. URL <https://doi.org/10.1287/moor.1110.0516>.
- Tom Zahavy, Andre Barreto, Daniel J Mankowitz, Shaobo Hou, Brendan O’Donoghue, Iurii Kemaev, and Satinder Singh. Discovering a set of policies for the worst case reward. In *International Conference on Learning Representations*, 2021. URL <https://openreview.net/forum?id=PUkhWz65dy5>.

A Appendix

A.1 The FR as an Exploration Bonus

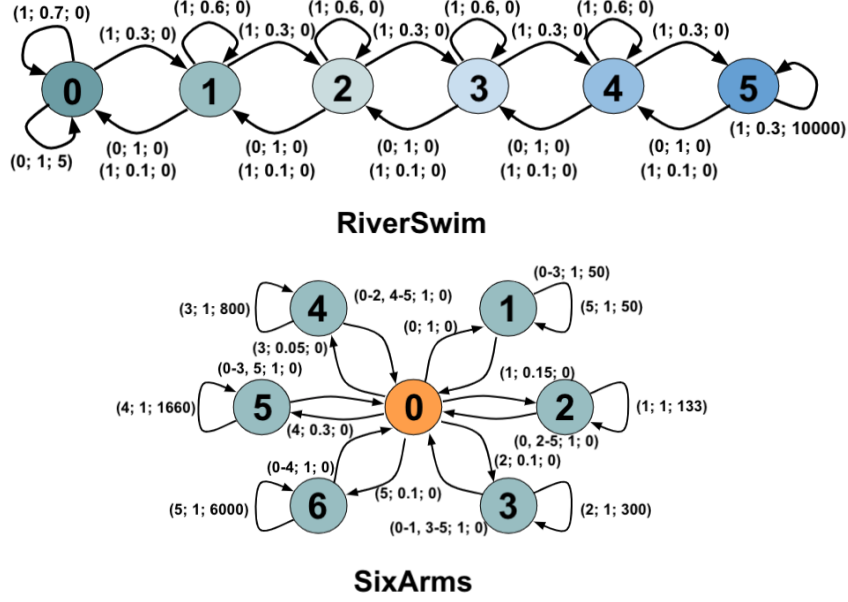


Figure 9: **Tabular environments for exploration.** The tuples marking each transition denote (action id(s); probability; reward). In RiverSwim, the agent starts in either state 1 or state 2 with equal probability, while for SixArms the agent always starts in state 0.

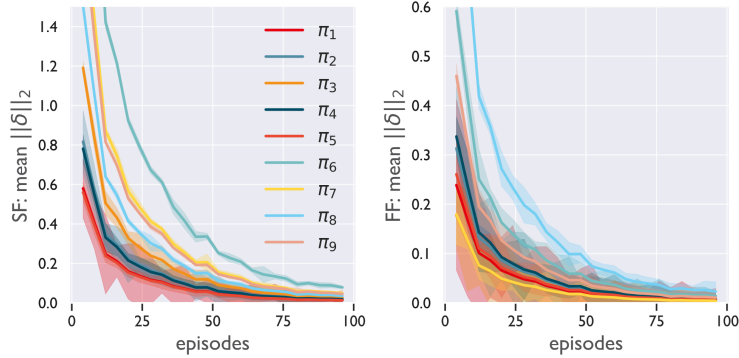


Figure 10: **FF and SF learning curves for continuous MountainCar.** Results averaged over 20 runs. Shading represents one standard deviation.

A.2 Additional Experimental Details

All experiments were performed on a single 8-core CPU.

MountainCar experiment In our version of the task, the feature representations are learned in a rewardless environment, and at test time the reward may be located at any location along the righthand hill. We evaluate the performance of a set of policies $\Pi = \{\pi_i\}$ with a constant magnitude of acceleration and which accelerate in the opposite direction from their current displacement when at rest and in the direction of their current velocity otherwise (see Python code below for details). That is, each π_i will swing back and forth along the track with a fixed power coefficient a_i . For each possible reward location along the righthand hill, then, the best policy from among this set is the one whose degree of acceleration is such that it arrives at the reward location in the fewest time steps. There is a natural tradeoff—too little acceleration and the cart will not

reach the required height. Too much, and time will be wasted traveling too far up the lefthand hill and then reversing momentum back to the right.

We hypothesized that the FF would be a natural representation for this task, as it would not count the repeated state visits each policy experiences as it swings back and forth to gain momentum.

We defined a set of policies with acceleration magnitudes $|a_i| = 0.1i$ for $i = 1, \dots, 9$, and learned both their SFs and FFs via TD learning on an "empty" environment without rewards over the course of 100 episodes, each consisting of 200 time steps, with the SFs using just the simple RBF feature functions without thresholds. Python code for the policy class is shown below.

```

1  class FixedPolicy:
2
3  def __init__(self, a):
4      # set fixed acceleration/power
5      self.a = a
6
7  def get_action(self, pos, vel):
8
9      if vel == 0:
10         # if stopped, accelerate to the opposite end of the environment
11         action = -sign(pos) * self.a
12     else:
13         # otherwise, continue in the current direction of motion
14         action = sign(vel) * self.a
15
16     return action

```

We repeated this process for 20 runs, with the plots in Fig. 10 showing the means and standard deviations of the TD learning curves across runs. For the FFs, the thresholds were constant across features at $\theta_d = \theta = 0.7$. Because of the nature of the environment, all of the policies spent a significant portion of time coasting back and forth between the hills, causing their SFs to accumulate in magnitude each time states were revisited.

Given the learned representations, we then tested them by using them as features for policy evaluation in different tasks, with each task containing a different rewarded/absorbing state. Note that a crucial factor is that the representations were learned in the environment without absorbing states. This is natural, as in the real world reward may arise in the environment anywhere, and we'd like a representation that can be effective for any potential goal location.

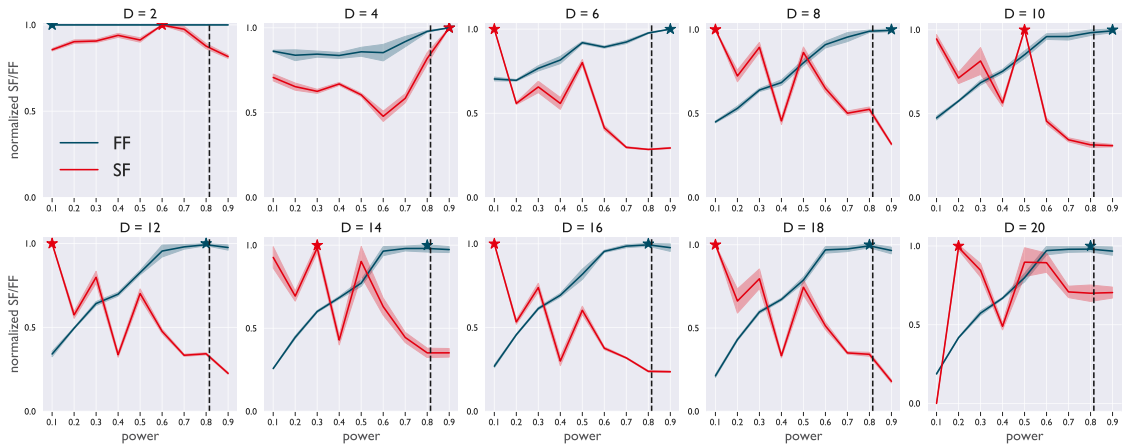


Figure 11: **The FF is robust to feature dimensionality.** FF and SF representation strengths for difference feature dimensionalities between the start and goal locations for an example goal in continuous MountainCar. The vertical dashed line marks the power of the optimal policy. We can see that for all but the coarsest feature representation, the FF is highest for the policy closest to the optimal.

Fig. 11 shows the value of the FF and SF at the start state for different policies with fixed power and for different feature dimensions (number of basis functions) in continuous MountainCar. The results show that the policies for which the FF is highest is closer in power to the optimal policy than for the policies at which the SF is greatest across all but the coarsest feature dimensionalities. This provides an indication of the robustness of the FF to the choice of feature dimensionality.

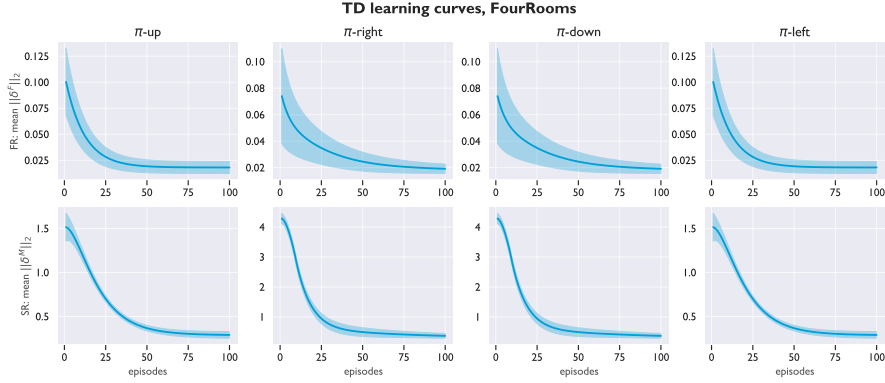


Figure 12: **FourRooms learning curves.** FourRooms base policies learning curves (average L2 norm of TD errors over 10 runs; shaded area is one standard deviation); top row is for FRs , bottom is for SRs.

FourRoom experiments The FourRoom environment we used was defined on an 11×11 gridworld in which the agent started in the bottom left corner and moved to a known goal state. The action space was $\mathcal{A} = \{\text{up}, \text{right}, \text{down}, \text{left}\}$ with four base policies each corresponding to one of the basic actions. TD Learning curves for the base policies are depicted in Fig. 12. Once reaching the goal, a new goal was uniformly randomly sampled from the non-walled states. At each time step, the agent received as state input only the index of the next square it would occupy. Each achieved goal netted a reward of $+50$, hitting a wall incurred a penalty of -1 and kept the agent in the same place, and every other action resulted in 0 reward. There were 75 timesteps per episode—the agent had to reach as many goals as possible within that limit. The discount factor γ was 0.95, and the FR learning rate was 0.05. In order to learn accurate FRs for each policy, each policy was run for multiple start states in the environment for 50 episodes prior to training. FRP (for different values of K), GPI, and VI were each run for 100 episodes. VI was given the true transition matrix and reward vector in each case. In the stochastic case, for each level of transition noise $\epsilon = 0.0, 0.1, 0.2, \dots, 1.0$, both VI and FRP were run to convergence (≈ 180 iterations for VI, 3 iterations for FRP) and then tested for 100 episodes.

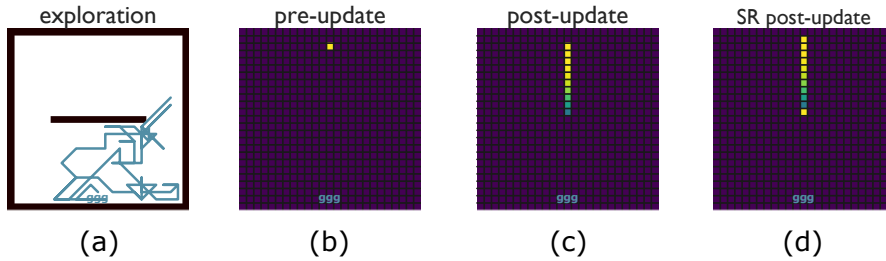


Figure 13: **Exploration and escape** (a) A sample trajectory from the “exploration phase” starting from the shelter. (b) Because the agent starts from the shelter during exploration, the first time it is tested starting from the top of the grid, its FR for the **down** policy for that state is still at initialization. (c) After updating its FR during testing and further exploration, the FR for the **down** policy from the start state is accurate, stopping at the barrier. (d) We can see that if we were to use the SR instead, the value in the state above the wall would accumulate when it gets stuck.

Escape experiments The escape experiments were modeled as a 25×25 gridworld with eight available actions,

$$\mathcal{A} = \{\text{up}, \text{right}, \text{down}, \text{left}, \text{up-right}, \text{down-right}, \text{down-left}, \text{up-left}\} \quad (24)$$

and a barrier one-half the width of the grid optionally present in the center of the room. The discount factor γ was 0.99, and the FR learning rate was 0.05. In test settings, the agent started in the top central state of the grid, with a single goal state directly opposite. At each time step, the agent receives only a number corresponding to the index of its current state as input. The base policy set Π consisted of eight policies, one for each action in \mathcal{A} . Escape trials had a maximum of 50 steps, with termination if the agent reached the goal state. In (Shamash et al., 2021), mice were allowed to explore the room starting from the shelter location. Accordingly, during “exploration phases,” the agent started in the goal state and randomly selected a base

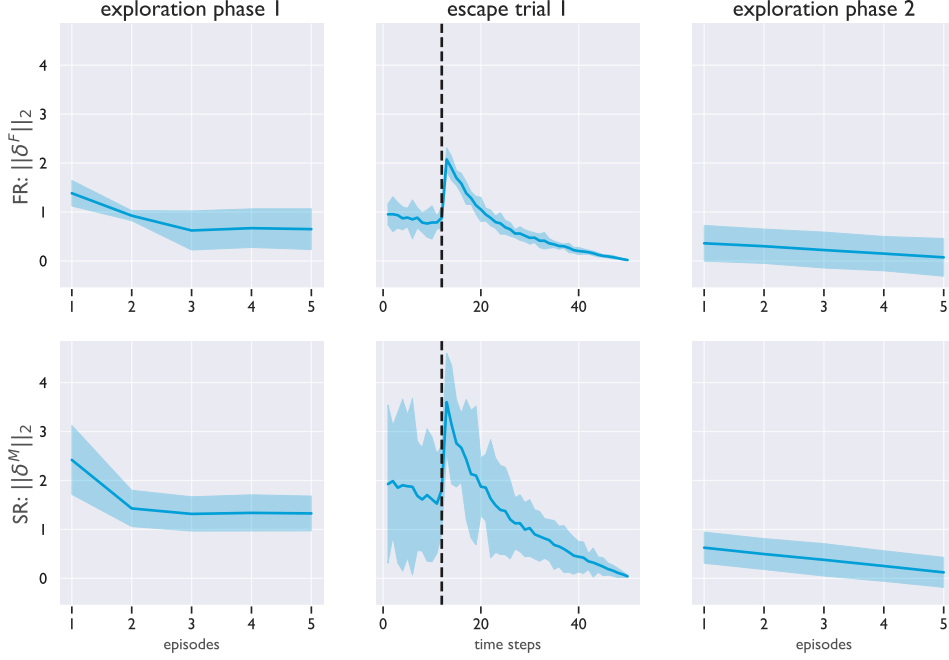


Figure 14: **Escape learning curves.** Learning curves (norms of TD errors) for the first exploration phase, the first escape trial, and the second exploration phase for the "down" policy. The vertical dotted lines in the escape trial mark the time step at which the agent encounters the barrier. This causes a temporary jump in the TD errors, as representation learning did not reflect the wall at this point. The top row consists of FR results and the bottom row is from SRs, averaged over 10 runs. The shading represents one standard deviation.

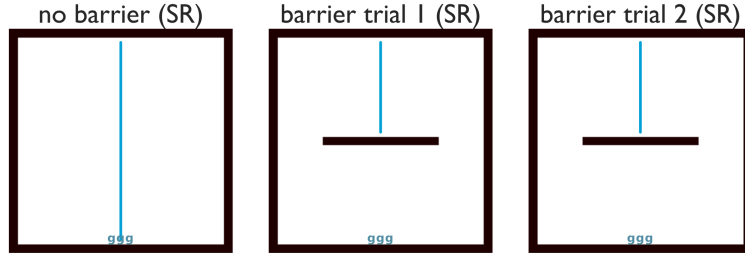


Figure 15: **An SR cannot effectively escape under the same conditions as an FR agent.**

policy at each time step, after which it updated the corresponding FR. Each exploration phase consisted of 5 episodes—a sample trajectory is shown in Fig. 13(a). After the first exploration phase, the agent started from the canonical start state and ran FRP to reach the goal state. Because most of its experience was in the lower half of the grid, the FRs for the upper half were incomplete (Fig. 13(b)), and we hypothesized that in this case, the mouse should either i) default to a policy which would take it to the shelter in the area of the room which it knew well (the **down** policy) or ii) default to a policy which would simply take it away from the threat (again the **down** policy). During the first escape trial, the agent selects the **down** policy repeatedly, continuing to update its FRs during the testing phase. Upon reaching the wall and getting stuck, the FR for the **down** policy is eventually updated enough that re-planning with FRP produces a path around the barrier. After updating its FR during the first escape trial and during another exploration period, the FRs for the upper half of the grid are more accurate (Fig. 13(c)) and running FRP again from the start state produces a faster path around the barrier on the second escape trial. TD learning curves for the experiment (repeated with the SR for completeness) are plotted in Fig. 14.

For completeness, we repeated this experiment with the SR. In this case, the planning algorithm is ill-defined for $K > 0$, so we default to GPI ($K = 0$). As expected, without the barrier, the **down** policy is selected and the goal is reached (Fig. 15, left). However, when there is a barrier, while the SR updates when the agent hits it (Fig. 12), since there is no single policy that can reach the shelter, GPI fails to find a path around the barrier (Fig. 15, middle, right).

A.3 Additional Proofs

Below is the proof of Proposition 3.1, which is restated below.

Proposition 3.1 (Contraction). *Let \mathcal{G}^π be the operator as defined in Definition 3.2 for some stationary policy π . Then for any two matrices $F, F' \in \mathbb{R}^{|S| \times |S|}$,*

$$|\mathcal{G}^\pi F(s, s') - \mathcal{G}^\pi F'(s, s')| \leq \gamma |F(s, s') - F'(s, s')|, \quad (25)$$

with the difference equal to zero for $s = s'$.

Proof. For $s \neq s'$ we have

$$|(\mathcal{G}^\pi - \mathcal{G}^\pi F')_{s, s'}| = \gamma |(P^\pi F - P^\pi F')_{s, s'}| = \gamma |P^\pi (F - F')_{s, s'}| \leq \gamma |(F - F')_{s, s'}|,$$

where we use the notation $X_{s, s'}$ to mean $X(s, s')$, and the inequality is due to the fact that every element of $P^\pi(F - F')$ is a convex average of $F - F'$. For $s = s'$, we trivially have $|(\mathcal{G}^\pi F - \mathcal{G}^\pi F')_{s, s}| = |1 - 1| = 0$. \square

Below is the proof of Proposition 4.1, which is restated below.

Proposition 4.1 (Planning optimality). *Consider a finite MDP with deterministic transitions, a single goal state s_g , and a base policy set Π composed of deterministic policies $\pi : \mathcal{S} \rightarrow \mathcal{A}$, $\forall \pi \in \Pi$. We make the following coverage assumption, there exists some sequence of policies that reaches s_g from a given start state s_0 . Under these conditions, Alg. 1 converges such that $\Gamma(s_0) = \gamma^{L_\Pi^*}$, where L_Π^* is the shortest path length from s_0 to s_g using $\pi \in \Pi$.*

Proof. Since the MDP is deterministic, we use a deterministic transition function $\rho : \mathcal{S} \times \mathcal{A} \rightarrow \mathcal{S}$. We proceed by induction on L_Π^* .

Base case: $L_\Pi^* = 1$

If $L_\Pi^* = 1$, s_0 must be one step from s_g . The coverage assumption guarantees that $\exists \pi \in \Pi$ such that $\rho(s_0, \pi(s_0)) = s_g$. Note also that when both the MDP and policies in Π are deterministic, $F^\pi(s, s') = \gamma^{L_\pi}$, where L_π is the number of steps from s to s' under π , and we use the abuse of notation $L_\pi = \infty$ if π does not reach s' from s .

Then following Alg. 1,

$$\begin{aligned} \Gamma_1(s_0) &= \max_{\pi \in \Pi} F^\pi(s_0, s_g) = \gamma \quad (\text{guaranteed by coverage of } \Pi) \\ \Gamma_1(s_g) &= \max_{\pi \in \Pi} F^\pi(s_g, s_g) = 1 \quad (\text{by definition of } F^\pi). \end{aligned}$$

Moreover,

$$\begin{aligned} \Gamma_2(s_0) &= \max_{\pi \in \Pi, s' \in \mathcal{S}} F^\pi(s_0, s') \Gamma_1(s') \\ &= \max_{\pi \in \Pi} \{F^\pi(s_0, s_0) \Gamma_1(s_0), F^\pi(s_0, s_g) \Gamma_1(s_g)\} \\ &= \max\{1 \cdot \gamma, \gamma \cdot 1\} \\ &= \gamma. \end{aligned}$$

Then $\Gamma_2(s) = \Gamma_1(s) \forall s$ and Alg. 1 terminates. Thus, $\Gamma(s_0) = \gamma = \gamma^{L_\Pi^*}$ and the base case holds.

Induction step: Assume Proposition 4.1 holds for $L_\Pi^* = L$

Given the induction assumption, we now need to show that Proposition 4.1 holds for $L_\Pi^* = L + 1$. By the induction and coverage assumptions, there must exist at least one state within one step of s_g that the agent can reach in L steps, such that the discount for this state or states is γ^L . Moreover, the coverage assumption guarantees that $\exists \pi \in \Pi$ such that for at least one such state s_L , $\rho(s_L, \pi(s_L)) = s_g$.

Then this problem reduces to the base case—that is, Alg. 1 will select the policy $\pi \in \Pi$ that transitions directly from s_L to s_g —and the proof is complete. \square

A.4 Explicit Planning

Below we describe a procedure for constructing an explicit plan using π^F and s^F .

Algorithm 2: ConstructPlan

```

1: input: goal state  $s_g$ , planning policy  $\pi^F$ , subgoals  $s^F$ 
2:  $\Lambda \leftarrow []$  ▷ init. plan
3:  $s \leftarrow s_0$  ▷ begin at start state
4: while  $s \neq s_g$  do
5:    $\Lambda.append((\pi^F(s), s^F(s)))$  ▷ add policy-subgoal pair for current state to plan
6:    $s \leftarrow s^F(s)$ 
7: end while
8: return  $\Lambda$ 

```

A.5 FRP with Multiple Goals

Here we consider the application of FRP to environments with multiple goals $\{g_1, \dots, g_n\}$. To find the shortest path between them given the base policy set Π , we first run FRP for each possible goal state in $\{g_i\}$, yielding an expected discount matrix $\Gamma^\Pi \in [0, 1]^{|\mathcal{S}| \times n}$, such that $\Gamma^\Pi(s, g_i)$ is the expected discount of the shortest path from state s to goal g_i . We denote by $g_\sigma = [s_0, \sigma(g_1), \sigma(g_2), \dots, \sigma(g_n)]$ a specific ordering of the goals in $\{g_i\}$ starting in s_0 . The expected discount of a sequence of goals is then

$$\Xi(g_\sigma) = \prod_{i=1}^n \Gamma^\Pi(g_\sigma(i-1), g_\sigma(i)), \quad (26)$$

with the optimal goal ordering g_{σ^*} given by

$$g_{\sigma^*} = \operatorname{argmax}_{g_\sigma \in G} \Xi(g_\sigma), \quad (27)$$

where G is the set of all possible permutations of $\{g_i\}$, of size $n!$. This is related to a form of the travelling salesman problem. Fortunately, in most settings we don't expect the number of goals n to be particularly large.

A.6 Connections to options

There are several important distinctions between FRP and planning within the options framework (Sutton et al., 1999). First, FRP doesn't require as input all possible policies and termination conditions, which could be prohibitively large to precompute, but rather only an arbitrary set of policies (sans termination conditions), for which, if the policies satisfy the coverage assumption, the algorithm is guaranteed to find the optimal path given the policies at hand. Second, it's important to note that the policy representations (FRs) are learned via TD updating rather than planned via DP—the FR learning and FRP were performed without knowledge of the transition dynamics, and the FRs can be reused across a given family of MDPs.

FRP can also be seen as related to the work of Silver & Ciosek (2012), which demonstrates that value iteration performed on top of a set of task-specific options converges more quickly than value iteration performed on the default state space of the MDP. One critical difference to note is that the FR/FRP is transferable to any MDP with shared transition dynamics. While value iteration on a set of options for a given MDP is more efficient than value iteration performed directly on the underlying MDP, this process must be repeated every time the reward function changes. However, the FR enables an implicit representation of the transition dynamics to be cached and reused. In the FourRooms experiments, for example, no additional computation was required each time the reward function changed, whereas VI had to be re-run every time a goal was reached.